Autophagy protects against active tuberculosis by suppressing bacterial burden and inflammation

Eliseo F. Castillo[a,1], Alexander Dekonenko[b,1], John Arko-Mensah[a], Michael A. Mandell[a], Nicolas Dupont[a], Shanya Jiang[a], Monica Delgado-Vargas[a], Graham S. Timmins[c], Dhruva Bhattacharya[a], Hongliang Yang[d], Julie Hutt[e], C. Rick Lyons[b], Karen M. Dobos[d], and Vojo Deretic[a,2]

Departments of [a]Molecular Genetics and Microbiology and [b]Internal Medicine and [c]College of Pharmacy, University of New Mexico Health Sciences Center, Albuquerque, NM 87131; [d]Department of Microbiology, Immunology and Pathology, College of Veterinary Medicine and Biomedical Sciences, Colorado State University, Fort Collins, CO 805235; and [e]Experimental Toxicology Division, Lovelace Respiratory Research Institute, Albuquerque, NM 87108

Edited* by Ralph R. Isberg, Howard Hughes Medical Institute and Tufts University School of Medicine, Boston, MA, and approved September 27, 2012 (received for review June 21, 2012)

Autophagy is a cell biological pathway affecting immune responses. In vitro, autophagy acts as a cell-autonomous defense against *Mycobacterium tuberculosis*, but its role in vivo is unknown. Here we show that autophagy plays a dual role against tuberculosis: antibacterial and anti-inflammatory. *M. tuberculosis* infection of Atg5$^{fl/fl}$ LysM-Cre^{+} mice relative to autophagy-proficient littermates resulted in increased bacillary burden and excessive pulmonary inflammation characterized by neutrophil infiltration and IL-17 response with increased IL-1α levels. Macrophages from uninfected Atg5$^{fl/fl}$ LysM-Cre^{+} mice displayed a cell-autonomous IL-1α hypersecretion phenotype, whereas T cells showed propensity toward IL-17 polarization during nonspecific activation or upon restimulation with mycobacterial antigens. Thus, autophagy acts in vivo by suppressing both *M. tuberculosis* growth and damaging inflammation.

Th17 response | calpain | inflammasome | macrophage

Autophagy is a fundamental cell biological process (1) with impact on aging, development, cancer, neurodegeneration, myodegeneration, metabolic disorders (2), idiopathic inflammatory diseases, and infection and immunity (3). Much of the physiological effects of autophagy are the result of degradative activities of autophagy (1), although biogenesis and secretory roles (4–6) of autophagy are beginning to be recognized (7). The execution of autophagy depends on factors collectively termed "Atg proteins," such as Atg5 (1) and Beclin 1 (Atg6) (8), whereas regulation of autophagy responds to various inputs via mammalian target of rapamycin (mTOR), including the presence of microbes (9), the TAB2/3–TAK1–IKK signaling axis (10), and processes downstream of pattern-recognition receptors and immune cytokine activation (3, 11–13).

In the context of its immunological functions, autophagy acts in four principal ways (14). (*i*) Autophagy cooperates with conventional pattern-recognition receptors (PRRs), such as Toll-like receptors, RIG-I–like receptors (RLRs), and NOD-like receptors, and acts as both a regulator (11, 12, 15, 16) and an effector of PRR signaling (17–19). (*ii*) Autophagy affects the presentation of cytosolic antigens in the context of MHC II molecules (20) in T-cell development, differentiation, polarization, and homeostasis (21, 22). (*iii*) Most recently, autophagy has been shown to contribute to both the negative (6, 7, 23–25) and positive (6, 7) regulation of unconventional secretion of the leaderless cytosolic proteins known as "alarmins," such as IL-1β and HMGB1. (*iv*) Autophagy can capture and eliminate intracellular microbes, including *Mycobacterium tuberculosis* (17, 26–29), which was one of the first two bacterial species (26, 30) to be recognized as targets for autophagic removal. This activity recently has been shown to depend on the recognition and capture of microbes by adaptors that represent a specialized subset of PRRs termed "sequestosome-like receptors" (SLRs) (31).

M. tuberculosis is one of the first microbes recognized as being subject to elimination by immunological autophagy by murine and human macrophages in ex vivo systems (17, 22, 26, 27, 29). Although it has been shown that macrophages from Atg5$^{fl/fl}$ LysM-Cre^{+} mice defective for autophagy in myeloid lineage fail to control *M. tuberculosis* H37Rv (32), the in vivo role of autophagy in controlling *M. tuberculosis* has not been reported. Given the compelling reasons for testing whether autophagy is involved in the control of *M. tuberculosis* in vivo, we used a mouse model of tuberculosis with transgenic mice deficient in Atg5 in the myeloid lineage, including macrophages, a cell type parasitized by *M. tuberculosis* (33). We demonstrate that autophagy controls tuberculosis infection in vivo and show a parallel role of autophagy in preventing excessive inflammatory reactions in the host.

Results

Autophagy Protects Mice from *M. tuberculosis*. The in vivo role of autophagy was investigated by selective genetic deletion of Atg5 in myeloid cells (which include macrophages and granulocytes); macrophages were of principal interest as the cells both successfully parasitized by intracellular *M. tuberculosis* (33) and targeted by protective immune responses. We used the previously reported conditional gene-knockout mouse model Atg5$^{fl/fl}$ LysM-Cre^{+} with Atg5 deletion in myeloid lineage (34). The Atg5^{+} mice (Atg5$^{fl/fl}$ LysM-Cre^{-}) and their Atg5$^{fl/fl}$ LysM-Cre^{+} littermates, previously characterized for lack of Atg5 and autophagy in macrophages (6), were subjected to aerogenic infection with low-dose ($10e^{2}$–$10e^{3}$ cfu) virulent *M. tuberculosis* H37Rv. An increase in bacterial burden (Fig. 1*A*) and weight loss (Fig. 1*B*) were observed in Atg5$^{fl/fl}$ LysM-Cre^{+} mice compared with Atg5$^{fl/fl}$ LysM-Cre^{-} littermates. The lung pathology in Atg5$^{fl/fl}$ LysM-Cre^{+} mice was remarkable for gross tubercle lesions, in contrast to the smaller infected foci in the lungs of Atg5^{+} animals (Fig. 1*C*). Atg5$^{fl/fl}$ LysM-Cre^{+} lung tissue revealed extensive necrotic centers (Fig. 1*D*, *i–iv*) with an increase in the percent of involved lung area and total lung weight (*SI Appendix*, Fig. S1 *A* and *B*) and a differential increase in polymorphonuclear

Author contributions: E.F.C., A.D., J.A.-M., M.A.M., N.D., S.J., M.D.-V., C.R.L., and V.D. designed research; E.F.C., A.D., J.A.-M., M.A.M., N.D., S.J., M.D.-V., and D.B. performed research; H.Y. and K.M.D. contributed new reagents/analytic tools; E.F.C., A.D., J.A.-M., M.A.M., N.D., S.J., M.D.-V., G.S.T., D.B., J.H., and V.D. analyzed data; and E.F.C. and V.D. wrote the paper.

The authors declare no conflict of interest.

*This Direct Submission article had a prearranged editor.

Freely available online through the PNAS open access option.

[1]These authors contributed equally to this work.

[2]To whom correspondence should be addressed. E-mail: vderetic@salud.unm.edu.

See Author Summary on page 18645 (volume 109, number 46).

This article contains supporting information online at www.pnas.org/lookup/suppl/doi:10.1073/pnas.1210500109/-/DCSupplemental.

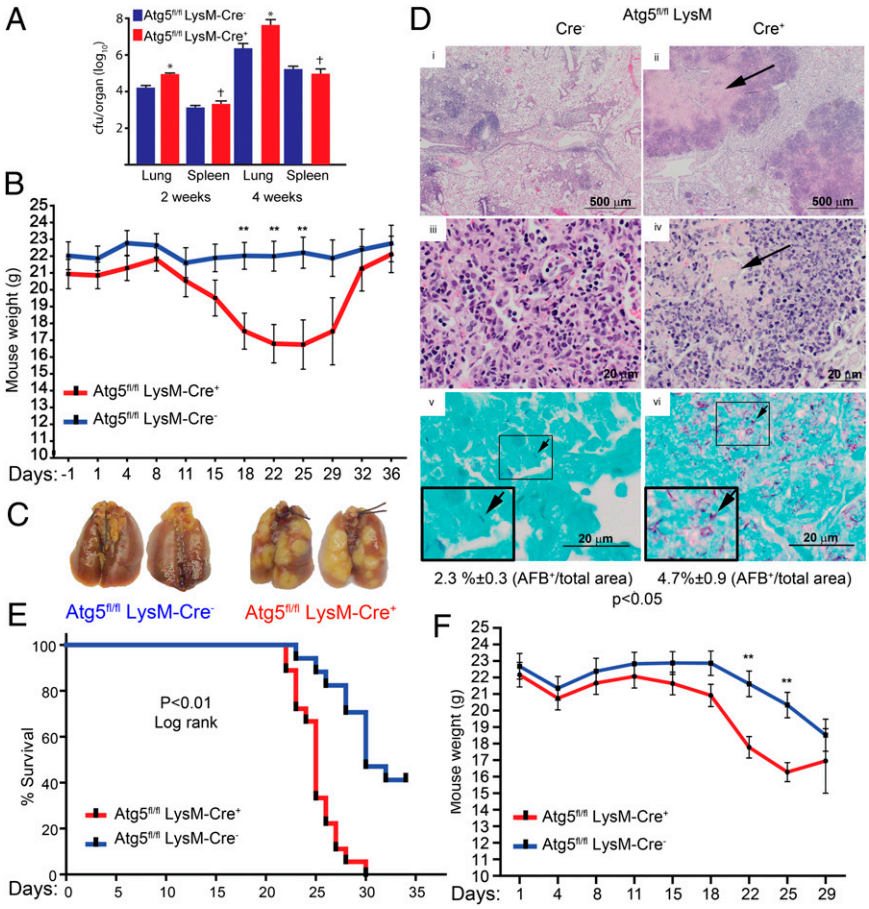

Fig. 1. Autophagy protects from excessive inflammation in a mouse model of tuberculosis infection. (*A*) Bacterial burden (cfu) in organs of Atg5$^{fl/fl}$ LysM-Cre^{+} and Atg5$^{fl/fl}$ LysM-Cre^{-} mice infected aerogenously with low-dose *M. tuberculosis* H37Rv [3 × 10e^{2} cfu (±30%) of initial bacterial deposition per lung following exposure to the infectious inoculum]. The data shown are representative of more than three independent low-dose experiments. (*B*) Weight loss in Atg5$^{fl/fl}$ LysM-Cre^{+} and Atg5$^{fl/fl}$ LysM-Cre^{-} mice infected with low-dose *M. tuberculosis* H37Rv. (*C*) Gross lung pathology (low dose). (*D*) Lung histological sections (low dose, day 36). (*i–iv*) H&E staining. Arrows indicate necrotic lesions. (*v* and *vi*) Acid-fast staining. Arrows indicate bacilli. (*Insets*) Enlarged views of boxed areas. AFB, acid-fast bacilli. (*E*) Survival of Atg5$^{fl/fl}$ LysM-Cre^{-} and -Cre^{+} mice infected with high-dose *M. tuberculosis* H37Rv (Kaplan–Meier survival analysis, log-rank method). (*F*) Weight loss in Atg5$^{fl/fl}$ LysM-Cre^{-} and -Cre^{+} mice infected with high-dose *M. tuberculosis* H37Rv (10e^{4} cfu per lung). When not otherwise specified, data are shown as mean ± SE; $*P < 0.05$, $**P < 0.01$, $^{\dagger}P > 0.05$ (ANOVA; $n \geq 3$).

(PMN) leukocytes (Ly6G^{+}) (*SI Appendix*, Fig. S1 *C–E*). Acid-fast bacilli per unit area were twofold higher in lung sections from Atg5$^{fl/fl}$ LysM-Cre^{+} mice than in lung sections from Atg5$^{fl/fl}$ LysM-Cre^{-} mice (Fig. 1*D*, *v* and *vi*). In keeping with the well-known general resistance of mice to tuberculosis, neither group of mice succumbed to the infection in short term (36 d). A 10-fold higher infection dose (10e^{4} cfu) resulted in animal mortality with accelerated deaths (along with continuing weight loss) among Atg5$^{fl/fl}$ LysM-Cre^{+} mice relative to their Atg5$^{fl/fl}$ LysM-Cre^{-} littermates, starting 3 wk postinfection (Fig. 1 *E* and *F*). These data indicate that Atg5$^{fl/fl}$ LysM-Cre^{+} mice are more susceptible to *M. tuberculosis* infection over a range of infectious doses and also suggest that the differences in lung pathology exceed the observed differences in bacterial burden.

Atg5 Deficiency in Myeloid Lineage Results in Excessive Inflammatory Response During Infection and Reflects, in Part, the Elevated Basal Markers of Inflammation. The cytokine profile in the lungs of *M. tuberculosis*-infected animals was remarkable for significant increases in IL-1α, IL-12, and CXCL1 in the Atg5$^{fl/fl}$ LysM-Cre^{+} lungs relative to -Cre^{-} littermates (Fig. 2 *A–C*). Additionally, IL-17 was elevated in infected mice with disabled autophagy in myeloid cells (Fig. 2*D* and *SI Appendix*, Fig. S2*A*). No differences were observed in the lungs of infected Atg5$^{fl/fl}$ LysM-Cre^{+} vs. -Cre^{-} mice for IFN-γ and TNF-α, [the well-established antituberculosis cytokines (35)], IL-4 [a cytokine known to inhibit autophagy ex vivo (22)], IL-6, and MIP-1β (*SI Appendix*, Fig. S2 *B–F*). Some increases in GM-CSF and IL-1β were detected in infected Atg5$^{fl/fl}$ LysM-Cre^{+} mice as compared with -Cre^{-} animals, but the absolute levels of IL-1β were much lower than the levels of IL-1α (*SI Appendix*, Fig. S2 *G* and *H*).

The uninfected Atg5$^{fl/fl}$ LysM-Cre^{+} and -Cre^{-} animals did not display signs of morbidity, overt disease, or discomfort per standards of veterinary care or differences in mortality. However, IL-1α was detectable at low basal levels even in the lungs of uninfected mice and was higher in Atg5$^{fl/fl}$ LysM-Cre^{+} mice than in Atg5$^{fl/fl}$ LysM-Cre^{-} littermates (*SI Appendix*, Fig. S3*A*). Increased basal levels of CXCL1 were observed in the lungs of Atg5$^{fl/fl}$ LysM-Cre^{+} mice compared to lungs from -Cre^{-} mice (*SI Appendix*, Fig. S3*B*), whereas IL-12p70 levels were equal in both uninfected animal groups (*SI Appendix*, Fig. S3*C*). IL-1β and IL-17 were below the limits of detection in the lungs of both uninfected Atg5$^{fl/fl}$ LysM-Cre^{+} and uninfected -Cre^{-} mice (*SI Appendix*, Fig. S3 *D* and *E*). Thus, some components of the cytokine profiles seen during infection (notably IL-1α and CXCL1) were present at low levels in uninfected animals.

In uninfected Atg5$^{fl/fl}$ LysM-Cre^{+} and -Cre^{-} mice, similar numbers of cells expressing macrophage markers (F4/80^{+} CD11b^{+};

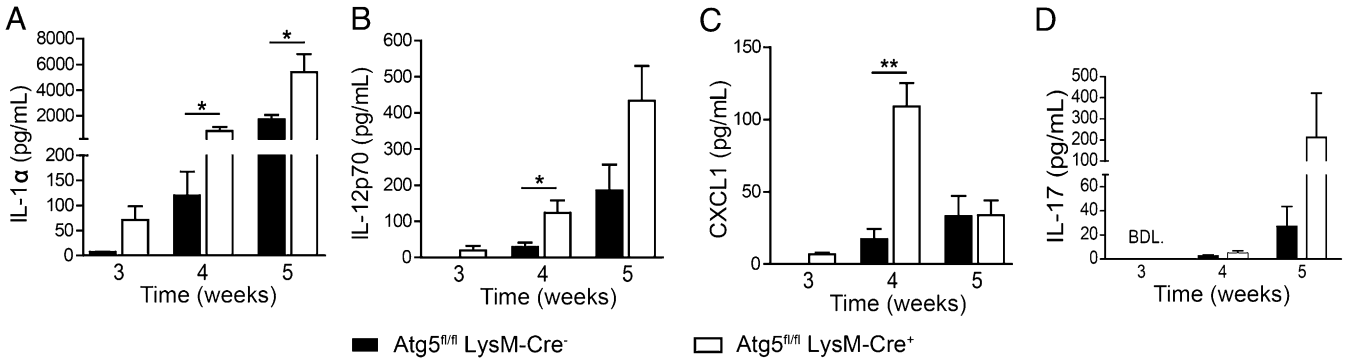

Fig. 2. Multiplex cytokine detection by Luminex in the lungs of Atg5$^{fl/fl}$ LysM-Cre^{-} and -Cre^{+} mice infected with low-dose *M. tuberculosis* H37Rv shows inflammatory cytokines are increased in Atg5$^{fl/fl}$ LysM-Cre^{+} mice. See *SI Appendix*, Fig. S2 for additional cytokines. BDL, below detection limit. Data are shown as mean ± SE; $^{*}P < 0.05$, $^{**}P < 0.01$, $^{\dagger}P > 0.05$ (*t* test; $n \geq 3$). Data in *D* represent the mean (± range) from a single cohort of infected mice. (See *SI Appendix*, Fig. S2*A* for pooled IL-17 data.)

lineage-negative CD3^{-} CD19^{-}) were detected in the lungs and bone marrow (*SI Appendix*, Fig. S3 *F* and *G*). However, unlike samples from their autophagy-competent littermates, a fraction of lung macrophages obtained from uninfected Atg5$^{fl/fl}$ LysM-Cre^{+} mice displayed activated phenotype (*SI Appendix*, Fig. S3*H*). Depending on the marker, 3–20% of Atg5$^{fl/fl}$ LysM-Cre^{+} macrophages had increased expression of MHC class II, DEC205, and CD86. An indication of increased CD11b^{+} F4/80^{-} cell numbers was observed in uninfected Atg5$^{fl/fl}$ LysM-Cre^{+} lungs (*SI Appendix*, Fig. S3*F*, *Top Left Quadrant*). Further examination revealed that these cells were Ly6G^{+} (1a8 clone) PMN granulocytes (neutrophils) (*SI Appendix*, Fig. S3*I*). This increase in total PMN number was observed only in the lungs, because bone marrow PMN numbers were comparable in the two groups of mice (*SI Appendix*, Fig. S3*J*). The innate immune cell analyses in uninfected animals, along with the cytokine data, indicate that the lungs of Atg5$^{fl/fl}$ LysM-Cre^{+} mice have elevated markers of immune activation under basal conditions as compared with their Atg5$^{fl/fl}$ LysM-Cre^{-} littermates. Thus, autophagy in myeloid cells of the lung, a peripheral organ where continual immune surveillance is necessary, maintains a homeostatic balance of immune cells and their activation states, a process that was perturbed in Atg5$^{fl/fl}$ LysM-Cre^{+} mice even before *M. tuberculosis* exposure.

Functional Autophagic Machinery in Myeloid Lineage Affects CD4 T-Cell Activation and IL-17 Response in Uninfected Animals. The PMN infiltrates, cytokines, and elevated IL-17 levels in the infected animals suggest elements of a Th17 response (36, 37). In the absence of infection, the fraction of lung CD4 and CD8 T cells with an activated/memory phenotype (CD44^{high}; Fig. 3*A*) was increased significantly in uninfected Atg5$^{fl/fl}$ LysM-Cre^{+} mice relative to uninfected Atg5$^{fl/fl}$ LysM-Cre^{-} littermates. We next stimulated total leukocytes from the lungs of uninfected mice with phorbol-12-myristate-13-acetate and ionomycin in the presence of protein secretion inhibitors and assessed intracellular levels of IL-17A and IFN-γ expressed by CD4 T cells. CD4 T cells from uninfected Atg5$^{fl/fl}$ LysM-Cre^{+} lungs, but not those from uninfected Atg5$^{fl/fl}$ LysM-Cre^{-} lungs, produced IL-17A (Fig. 3 *B* and *C*). There was no marked difference in the ability of CD4 T cells from the two sources to mount an IFN-γ response (Fig. 3 *D* and *E*). These findings show the propensity of CD4 T cells from uninfected Atg5$^{fl/fl}$ LysM-Cre^{+} mice to produce IL-17A upon stimulation, perhaps because of the increased IL-1α in the lung, reflecting the in vivo state of T cells induced by the lack of autophagy in myeloid cells.

Defective Autophagy in Myeloid Lineage of Atg5$^{fl/fl}$ LysM-Cre^{+} Mice Promotes the IL-17 Response to Defined *M. tuberculosis* Antigens by T Cells. The proinflammatory properties described above were investigated next using immunologically active components of *M. tuberculosis*. We used a mixture of five well-defined *M. tuberculosis* protein antigens (DnaK, GroEL, Rv009, Rv0569, and Rv0685) collectively referred to as "synthetic PPD" (38) in reference to the purified protein derivative (PPD) used clinically as a tuberculin skin test for evidence of recent tuberculosis infection or bacillus Calmette–Guérin vaccination. The synthetic PPD reproduces the anatomical and molecular properties of the tuberculin skin test but eliminates false-positive inflammatory reactions (seen in uninfected hosts) caused by the contaminating lipoglycans and carbohydrates resident in conventional PPD (38). Atg5$^{fl/fl}$ LysM-Cre^{+} and -Cre^{-} mice were injected peritoneally with live *Mycobacterium bovis* bacillus Calmette–Guérin, and the quality of their immune responses was evaluated 3 wk later. Mice were injected with the synthetic PPD or PBS (as control) in the hind footpad, and delayed-type hypersensitivity (DTH) induration was measured at 0, 2, 24, and 48 h post-inoculation (Fig. 4*A*). No differences between the autophagy-competent and mutant mice were observed at the 24 and 48 h time points. However, when splenocytes from the animals inoculated with bacillus Calmette–Guérin were restimulated ex vivo with synthetic PPD, IL-17A was detected at significantly higher levels in splenocytes from Atg5$^{fl/fl}$ LysM-Cre^{+} animals (Fig. 4*B*), but no differences were observed for typical Th1 and Th2 cytokine signatures (Fig. 4 *C*–*E*) indicating polarization to the IL-17–producing phenotype in Atg5$^{fl/fl}$ LysM-Cre^{+} mice.

Atg5 Deficiency Causes Cell-Autonomous Increase in IL-1α Secretion by Macrophages. The increased level of IL-17 in the lungs of infected Atg5$^{fl/fl}$ LysM-Cre^{+} animals is a product of T-cell polarization downstream of the changes in myeloid cells. The Atg5$^{fl/fl}$ LysM-Cre^{+} macrophages are known to possess increased inflammasome activation (6, 7, 23–25) downstream of reactive oxygen species (ROS) (16) and mitochondrial DNA (24) released from unkempt mitochondria in the absence of autophagy. A key proinflammatory cytokine activated via inflammasome, IL-1β, can lead to Th17 differentiation via IL-1 receptor signaling (37). However, IL-1β was present only in minor quantities in the lungs of Atg5$^{fl/fl}$ LysM-Cre^{+} animals infected with *M. tuberculosis* and was undetectable in uninfected lungs (*SI Appendix*, Figs. S2*H* and S3*D*). Nevertheless, IL-1α, which also signals via the IL-1 receptor, was a dominant cytokine elevated in both infected and uninfected Atg5$^{fl/fl}$ LysM-Cre^{+} lungs (Fig. 2*A* and *SI Appendix*, Fig. S2*A*). When we tested whether IL-1α can substitute for IL-1β (in combination with TGF-β and IL-6) in driving Th17 differ-

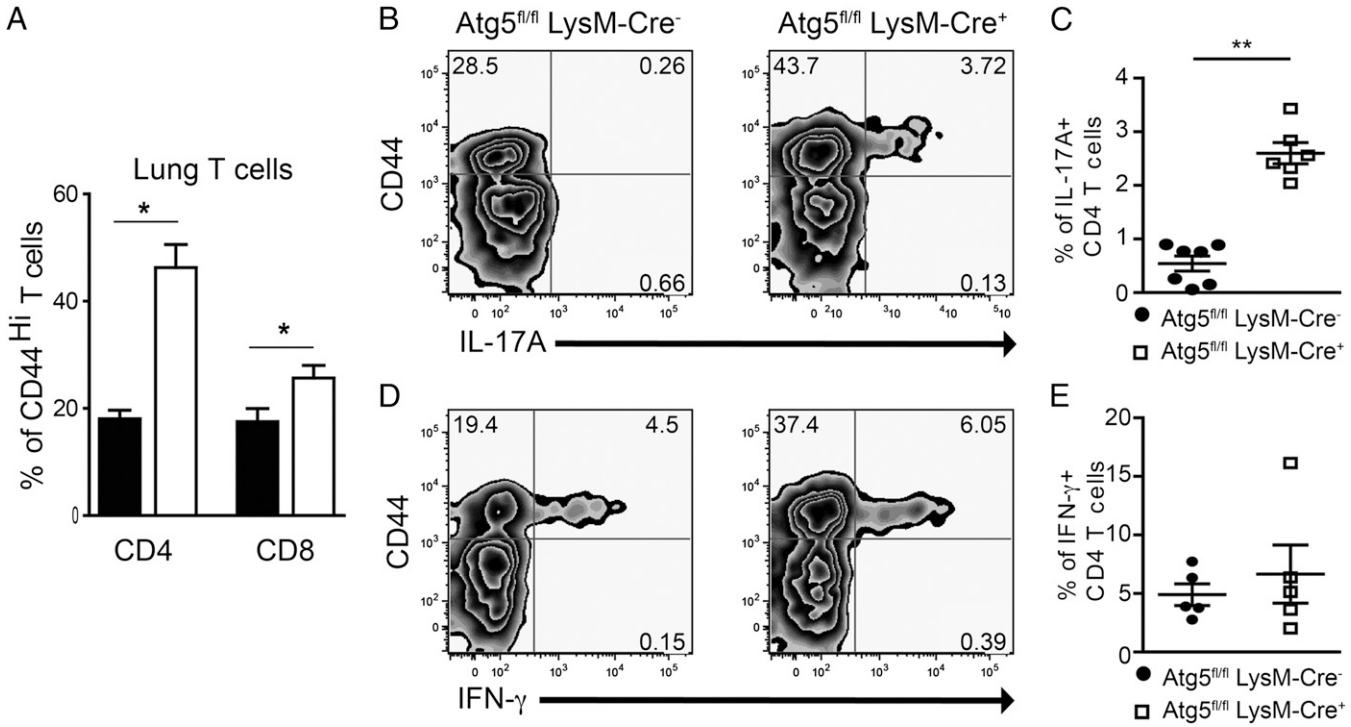

Fig. 3. Activated phenotype of CD4 T cells from uninfected Atg5$^{fl/fl}$ LysM-Cre^{+} mice and their propensity to undergo polarization into IL-17–producing cells. (*A*) CD44 expression on lung T cells. Graph displays the percent of CD44^{high} CD4 and CD8 T cells in the lung of uninfected Atg5$^{fl/fl}$ LysM-Cre^{-} and -Cre^{+} mice. The uninfected mice were 10–12 wk of age. (*B–D*) Intracellular levels of IL-17A (*B* and *C*) and IFN-γ (*D* and *E*) in CD44 T cells isolated from lungs of uninfected Atg5$^{fl/fl}$ LysM-Cre^{-} and -Cre^{+} mice and stimulated with phorbol 12-myristate 13-acetate and ionomycin ex vivo in the presence of brefeldin A and monensin. Data are shown as mean ± SE; $*P < 0.05$, $**P < 0.01$ (*t* test; $n \geq 3$).

entiation ex vivo, IL-1α showed a capacity to promote Th17 polarization (*SI Appendix*, Fig. S4 *C–F*).

In vitro-activated Atg5$^{fl/fl}$ LysM-Cre^{+} bone marrow macrophages (BMM) recapitulated the in vivo pattern of elevated secretion of IL-1α (along with CXCL1 and IL-12p70) relative to Atg5$^{fl/fl}$ LysM-Cre^{-} BMM (Fig. 5 *A–C*). The CXCL1 phenotype was likely secondary to IL-1 increase, because IL-1 receptor antagonist (IL-1RA) lowered CXCL1 levels (Fig. 5*D*). Differential release of IL-1α, which is a cytosolic protein, was not caused by changes in cell death or increased membrane permeability, because in vitro-activated BMM from Atg5$^{fl/fl}$ LysM-Cre^{+} and Atg5$^{fl/fl}$ LysM-Cre^{-} mice showed no difference in staining with 7-aminoactinomycin D (7-AAD) (Fig. 5*E*). These experiments, and additional data showing elevated secretion of IL-1α in the lungs of uninfected Atg5$^{fl/fl}$ LysM-Cre^{+} animals [whereas IL-12p70 and IL-1β were below detection levels in these mice (*SI Appendix*, Fig. S3 *D* and *E*)], singled out IL-1α as a potential pivot of the proinflammatory pathology observed with Atg5$^{fl/fl}$ LysM-Cre^{+} mice in the tuberculosis model. We could not test this conclusion in vivo, however, because IL-1α also plays a critical protective role against bacterial burden, as recently shown in IL-1α–knockout mice (39).

Cellular Mechanism for Increased Secretion of IL-1α by Autophagy-Deficient Macrophages Is Inflammasome Independent. We wanted to understand the cellular mechanism of the IL-1α hypersecretion phenotype in Atg5$^{fl/fl}$ LysM-Cre^{+} macrophages. Autophagy was confirmed as a negative regulator of IL-1α release by pharmacologically manipulating autophagy in Atg5$^{fl/fl}$ LysM-Cre^{-} BMM. The induction of autophagy with rapamycin in autophagy-competent macrophages reduced the amount of IL-1α being secreted (Fig. 5*F*), paralleling the effects on IL-1β (*SI Appendix*, Fig. S5*A*), a cytokine whose secretion we (6) and others (23, 24) previously have reported to be affected by autophagy. Conversely, when Atg5$^{fl/fl}$ LysM-Cre^{-} BMM were treated with 3-methyladenine (3MA), an inhibitor of autophagosome formation, the levels of IL-1α were increased significantly (Fig. 5*E*). As a control, autophagy-deficient Atg5$^{fl/fl}$ LysM-Cre^{+} BMM showed no response in IL-1α secretion to these pharmacological agents (*SI Appendix*, Fig. S5*B*). An effect similar to 3MA was observed upon treatment of Atg5$^{fl/fl}$ LysM-Cre^{-} BMM with bafilomycin A1 (Baf A1), an inhibitor of autophagic flux (Fig. 5*G*).

We next considered multiple levels at which absence of autophagy could result in elevated IL-1α secretion. The autophagic adaptor protein p62, which is consumed during autophagy (40) and is the founding member of the SLR family of PRR (31), also functions prominently in innate immunity signaling (41). It accumulates in the absence of autophagy and has been shown to perturb NF-κB responses and cytokine secretion (41, 42). Because IL-1α expression is controlled by NF-κB (43), we tested whether p62-mediated NF-κB activation could be the cause of elevated IL-1α expression. However, knocking down p62 via siRNA in Atg5$^{fl/fl}$ LysM-Cre^{+} BMM (*SI Appendix*, Fig. S6*A*) did not abrogate the elevated IL-1α secretion by these cells (*SI Appendix*, Fig. S6*B*). Knocking down Atg5 in BMM from p62$^{-/-}$ knockout mice still caused more (albeit less pronounced, because of residual Atg5 levels) IL-1α secretion than in the scrambled siRNA control (*SI Appendix*, Fig. S6*C*). Finally, no increase in IL-1α mRNA levels was detected in Atg5$^{fl/fl}$ LysM-Cre^{+} BMM relative to Atg5$^{fl/fl}$ LysM-Cre^{-} BMM (*SI Appendix*, Fig. S6*D*). Thus, the p62–NF-κB axis does not contribute to the IL-1α phenotype in Atg5-deficient cells, and IL-1α expression is not transcriptionally activated in Atg5$^{fl/fl}$ LysM-Cre^{+} macrophages. We next considered whether IL-1α was a direct target for removal by autophagic organelles. Endogenous LC3 and IL-1α did not colocalize (*SI Appendix*, Fig. S6*E*, *Left and Center*

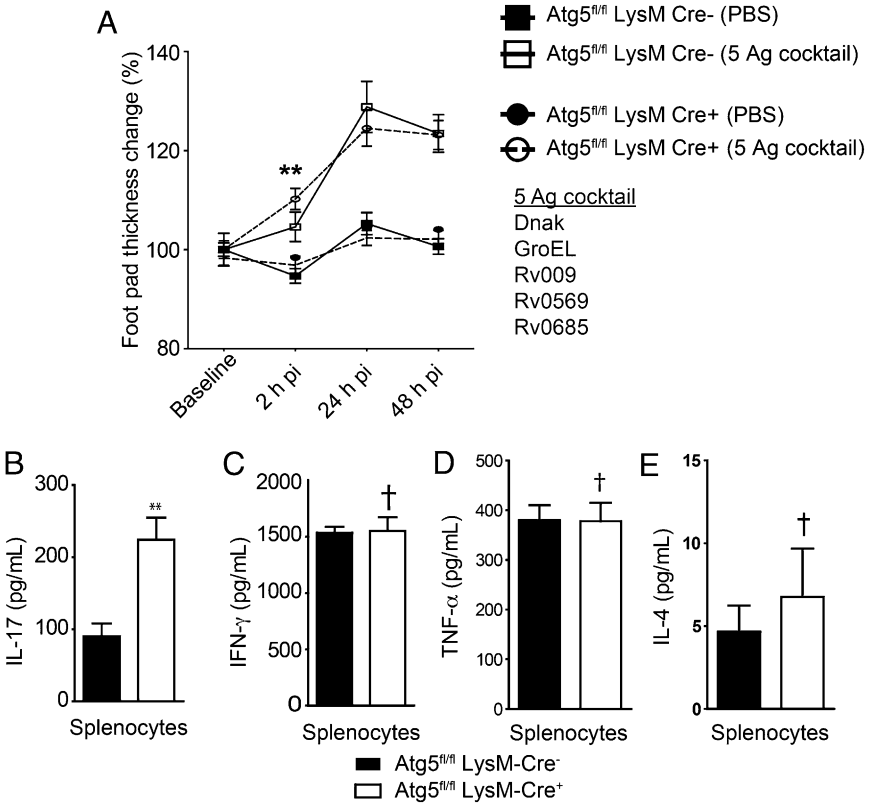

Fig. 4. In vivo and ex vivo immune response to defined *M. tuberculosis* antigens of Atg5$^{fl/fl}$ LysM-Cre^{+} mice and IL-17 production by their splenocytes upon ex vivo restimulation. (*A*) DTH reaction (footpad induration) at day 21 postinfection in Atg5$^{fl/fl}$ LysM-Cre^{-} and -Cre^{+} mice infected i.p. with bacillus Calmette–Guérin. Mice were injected in the footpad with synthetic PPD. Data are shown as percent change in footpad thickness upon challenge with the synthetic PPD relative to the contralateral, PBS-challenged footpad. (*B–E*) Cytokine production by splenocytes from Atg5$^{fl/fl}$ LysM-Cre^{-} and -Cre^{+} mice (day 23 after peritoneal injection of bacillus Calmette–Guérin) restimulated for 3 d ex vivo with synthetic PPD. All mice were 10–12 wk of age at the onset of the experiment. Data are shown as mean ± SE; $^{**}P < 0.01$, $^{\dagger}P > 0.05$ (*t* test; $n \geq 3$).

Images), displayed a negative Pearson's colocalization coefficient even upon treatment with Baf A1 (*SI Appendix*, Fig. S6*E*, *Graph*), and showed complete separation of respective profiles (*SI Appendix*, Fig. S6*E*, *Right Image*). Thus, IL-1α is unlikely to be a direct substrate for autophagic elimination.

Pathways leading to IL-1α secretion have been reported to use inflammasome components (44, 45) although, unlike IL-1β, intracellular IL-1α is not an enzymatic substrate for caspase 1. Atg5$^{fl/fl}$ LysM-Cre^{+} BMM showed elevated levels of p20 caspase 1 (its activated form) in comparison with Atg5$^{fl/fl}$ LysM-Cre^{-} BMM (*SI Appendix*, Fig. S6 *F* and *G*). The fluorochrome-labeled inhibitor of caspase (FLICA) assay confirmed increased enzymatically active caspase 1 in Atg5$^{fl/fl}$ LysM-Cre^{+} BMM compared with Atg5$^{fl/fl}$ LysM-Cre^{-} BMM (*SI Appendix*, Fig. S6*H*). In keeping with the potential role for inflammasome and caspase 1 in IL-1α release (44, 45), adding silica to macrophages increased their IL-1α output (Fig. 5*H*). However, both the basal and inflammasome agonist (silica)-induced levels of IL-1α released from macrophages were increased in Atg5$^{fl/fl}$ LysM-Cre^{+} BMM. Furthermore, when we tested whether this release was caspase 1 dependent, neither the enzymatic inhibitor of caspase 1, YVAD (Fig. 5*I*), nor caspase 1 knockdown (Fig. 5 *J–L*) decreased relative IL-1α output. We next tested whether the elevated IL-1α secretion by Atg5$^{fl/fl}$ LysM-Cre^{+} BMM was dependent on other inflammasome components. Knocking down the key inflammasome constituents ASC and NLRP3 did not diminish the IL-1α output of Atg5$^{fl/fl}$ LysM-Cre^{+} cells (Fig. 5*M*). These observations, although surprising, are in agreement with the recent report of an inflammasome/caspase 1-independent pathway for IL-1α secretion (46) and show that, although the inflammasome is activated in Atg5$^{fl/fl}$ LysM-Cre^{+} BMM, it is not responsible for the increase in IL-1α output.

Increased IL-1α in Atg5$^{fl/fl}$ LysM-Cre^{+} Macrophages Defines a ROS–Calpain Proinflammatory Pathway. We next searched for potential sources of IL-1α activation upstream of the inflammasome. ROS released by accumulated dysfunctional mitochondria in autophagy-deficient cells have been implicated in inflammatory signaling both during RLR response to viral products (16) and inflammasome activation in IL-1β production (23). Atg5$^{fl/fl}$ LysM-Cre^{+} BMM had elevated mitochondrial content (increased MitoTracker Green staining; *SI Appendix*, Fig. S7 *A–C*) accompanied by reduced mitochondrial polarization (decrease in MitoTracker Red staining; *SI Appendix*, Fig. S7 *D* and *E*). We tested whether ROS associated with the mitochondrial defect in other inflammatory signaling (16, 23) played a role in elevated IL-1α release from Atg5$^{fl/fl}$ LysM-Cre^{+} macrophages. The ROS inhibitor (2R,4R)-4-aminopyrrolidine-2, 4-dicarboxylate (APDC) abrogated excessive IL-1α (Fig. 5*O*). In keeping with the previous reports (23), APDC also inhibited excessive IL-1β release from Atg5$^{fl/fl}$ LysM-Cre^{+} BMM (Fig. 5*P*). Thus, ROS are mediators leading to hypersecretion of both IL-1α and IL-1β by autophagy-deficient cells, but the machinery downstream of ROS differs for the two cytokines, because IL-1β depends on the inflammasome (23), whereas IL-1α, as shown here, does not.

ROS can lead to calpain activation (47, 48), although this pathway has not been implicated previously in inflammation. We used ALLN, a calpain inhibitor, to test whether calpain is in-

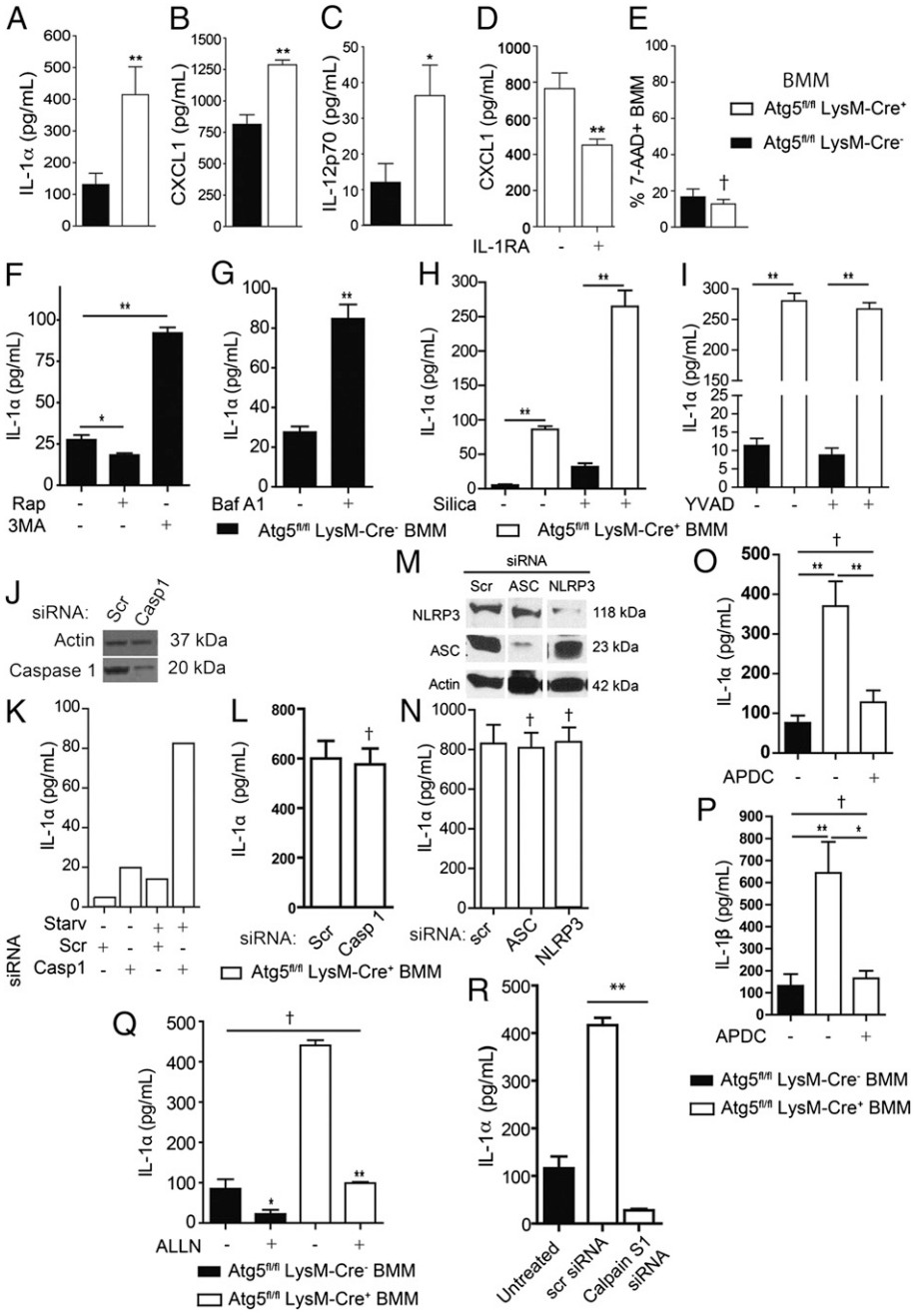

Fig. 5. Excess cytokine secretion is a cell-autonomous property of autophagy-deficient macrophages, and IL-1α hypersecretion by Atg5$^{fl/fl}$ LysM-Cre^{+} macrophages depends on reactive oxygen intermediates and calpain. (*A*–*C*) In vitro cytokine [IL-1α (*A*), CXCL1 (*B*), and IL-12p70 (*C*)] release (ELISA) from LPS- and IFN-γ–stimulated Atg5$^{fl/fl}$ LysM-Cre^{-} and -Cre^{+} BMM. (*D*) CXCL1 released (ELISA) from LPS- and IFN-γ–stimulated Atg5$^{fl/fl}$ LysM-Cre^{+} BMM in the absence of presence of IL-1RA (0.5 μg/mL). (*E*) Fraction (flow cytometry) of 7-AAD^{+} BMM after LPS and IFN-γ stimulation in vitro. (*F* and *G*) IL-1α (ELISA) released from LPS- and IFN-γ–stimulated Atg5$^{fl/fl}$ LysM-Cre^{-} BMM in the presence of 50 μg/mL rapamycin (Rap) or 10 mM 3-MA (*F*) or 100 nM Baf A1 (*G*) after 12 h of treatment. (*H*) IL-1α secretion during inflammasome activation. Atg5$^{fl/fl}$ LysM-Cre^{-} and -Cre^{+} BMM were pretreated overnight with LPS (100 ng/mL) and then were stimulated for 1 h in the absence or presence of the inflammasome agonist silica (250 μg/mL) in EBSS. (*I*) IL-1α secretion in the presence of caspase 1 inhibitor YVAD. Atg5$^{fl/fl}$ LysM-Cre^{-} and -Cre^{+} BMM were pretreated overnight with LPS (100 ng/mL) and then were stimulated for 1 h in the absence or presence of YVAD (50 μM) during inflammasome activation with silica as in *H*. (*J*–*L*) Effects of caspase 1 siRNA knockdown (immunoblot, *J*) on IL-1α release (graphs, *K* and *L*) from Atg5$^{fl/fl}$ LysM-Cre^{+} BMM. (*K*) IL-1α release was measured (ELISA) from LPS-stimulated and siRNA-treated Atg5$^{fl/fl}$ LysM-Cre^{+} BMM in full medium or EBSS (Starv) (*K*) or in full medium only (*L*). Casp 1, caspase 1 siRNA; Scr, scrambled siRNA (control). (*M* and *N*) Effects of NLRP3 and ASC siRNA knockdown (immunoblot, *M*) on IL-1α release (*N*). IL-1α release was measured (ELISA) from LPS- and IFN-γ–stimulated Atg5$^{fl/fl}$ LysM-Cre^{+} BMM knocked down with siRNA for inflammasome components ASC and NLRP3. (*O* and *P*) ROS inhibition and IL-1 secretion. IL-1α (*O*) and IL-1β (*P*) released (ELISA) from LPS- and IFN-γ–stimulated Atg5$^{fl/fl}$ LysM-Cre^{-} and -Cre^{+} BMM in the absence or presence of the ROS antagonist APDC (50 μM) after 12 h of incubation. (*Q*) Calpain and IL-1α hypersecretion phenotype. IL-1α (ELISA) released from LPS- and IFN-γ–stimulated Atg5$^{fl/fl}$ LysM-Cre^{-} and -Cre^{+} BMM in the absence or presence of the calpain inhibitor ALLN (100 μM) after 12 h of stimulation. (*R*) IL-1α release from LPS- and IFN-γ–stimulated Atg5$^{fl/fl}$ LysM-Cre^{-} BMM and Atg5$^{fl/fl}$ LysM-Cre^{+} BMM knocked down with siRNA for Calpain S1. Data are shown as mean ± SE; $^{*}P < 0.05$, $^{**}P < 0.01$, $^{\dagger}P > 0.05$ (*t* test; $n \geq 3$).

volved in the IL-1α hypersecretion phenotype of Atg5$^{fl/fl}$ LysM-Cre^{+} cells. ALLN treatment of Atg5$^{fl/fl}$ LysM-Cre^{+} completely inhibited the excess IL-1α production, normalizing its output to the levels seen with Atg5$^{fl/fl}$ LysM-Cre^{-} cells (Fig. 5*Q*). An siRNA knockdown of the common calpain regulatory (small) subunit Capns1, which forms heterodimers with and is required for function of the conventional murine calpains Capn1 and Capn2 (49), abrogated IL-1α hypersecretion (Fig. 5*R*). We also considered the possibility that calpain may be a target for degradation by autophagy; however, calpain levels were not different in Atg5$^{fl/fl}$ LysM-Cre^{+} vs. -Cre^{-} cells (*SI Appendix*, Fig. S6*F*), and calpain did not colocalize with autophagic organelles (*SI Appendix*, Fig. S6*G*). We conclude that the increase in IL-1α associated with the Atg5 defect in macrophages is caused by elevated ROS and depends not on the absolute levels of calpain but on its activation downstream of ROS, thus defining an additional proinflammatory pathway downstream of autophagy.

Discussion

This work demonstrates the in vivo role of autophagy in protection against tuberculosis. Along with the previous in vitro studies addressing the antimycobacterial effector mechanisms of autophagy (17, 22, 26–29, 50, 51), these results establish that autophagy is a bona fide barrier again tuberculosis. Autophagy protects against tissue necrosis and lung pathology, the hallmarks of active tuberculosis. This effect is not a simple consequence of increased bacillary loads but is compounded by the cell-autonomous action of autophagy in macrophage-driven inflammatory processes. Autophagy-deficient macrophages release excessive amounts of inflammatory mediators, such as IL-1α, even in the absence of infection. A model emerges whereby these mediators, when in excess, pivot inflammation with features of a Th17 response, neutrophilic infiltration, tissue necrosis, and organ damage, the main features of active tuberculosis and a contagious state of the host.

The mechanisms of cell-autonomous elimination of *M. tuberculosis* by autophagy have been studied extensively in vitro and include direct microbial digestion in autophagolysosomes (26), delivery of neo-antimicrobial peptides generated in autolysosomes to compartments harboring intracellular mycobacteria (27, 32, 50), and an interplay of autophagy with conventional antimicrobial peptides (28). Our previous work (32) highlighted the role of the SLR p62 in these processes, complementing the examples of other SLRs engaging an array of intracellular bacteria (31, 52–55) and viruses (56). In contrast to a preponderance of studies in vitro, autophagic control of microbes is not fully documented in vivo (34, 56). Altered intestinal tissue and Paneth cell function has been noted in response to microbial flora and viral coinfection in an Atg16L1 hypomorph mouse model of Crohn disease, a chronic inflammatory condition (57). In the animal model of protection against lethal Sindbis virus infection, the dominant contribution of autophagy was in preventing tissue damage independently of viral loads (56). These observations dovetail with the aspect of our study that shows autophagic protection against excessive inflammation and necrosis in the murine model of tuberculosis. We interpret our data and reports by others (23, 24, 57, 58) as evidence that partial seeds of endogenous inflammation and predisposition to hyperreactivity exist in autophagy-deficient uninfected animals. This predisposition is in keeping with the cell-autonomous IL-1α hypersecretion shown here and eventually leads to increased pathology in infected animals. Although leukocytes from uninfected Atg5$^{fl/fl}$ LysM-Cre^{+} animals show a propensity to polarize into IL-17 cells when tested ex vivo, IL-17 has been detected in vivo only in infected animals. Thus, the elevated IL-17 response represents a product of interactions between *M. tuberculosis* and a host defective for autophagy in myeloid cells.

The findings that a loss of autophagy in macrophages results in increased release of IL-1α and fosters an environment in which T cells produce IL-17 link autophagy with elements of the Th17 response. The associated elevated presence of neutrophils in the lungs of Atg5$^{fl/fl}$ LysM-Cre^{+} mice infected with *M. tuberculosis* may be linked to increased pathology. IL-17 and neutrophils play a complex role in tuberculosis (59) and confer both positive (60–62) and negative elements of protection (63–65). The latter aspect of the role of neutrophils in tuberculosis has been highlighted recently in patient cohort studies (66) and is compounded further by correlates between type I IFN (not addressed in our study) and different participating cells (66, 67). The pathogenic effects of neutrophils are notably manifested during repeat exposure to mycobacterial antigens (65) and at times when a lingering Th17 response does not give way to Th1 control (64) or is not suppressed by regulatory mechanisms (63). Our findings indicate that autophagy, when functional, curbs neutrophilic response, possibly at the time when it needs to be diminished (63–65).

All reports thus far (6, 23–25, 58, 68) agree that autophagy plays a negative role in inflammasome activation through a variety of triggers or additional mechanisms. Autophagy suppresses the basal level of inflammasome activation by continually removing (23, 24) endogenous sources of inflammasome agonists such as ROS and mitochondrial DNA (23, 24). Our findings with the ROS–calpain axis in IL-1α activation and findings by others regarding ROS–RLR signaling (16) expand these proinflammatory phenomena to noninflammasome pathways downstream of the accumulation of dysfunctional mitochondria and ROS in autophagy-deficient cells. Other changes with inflammatory consequences have been noted in mice with Atg5-deficient macrophages (57, 69).

Tuberculosis has been and remains one of the main global public health hazards further augmented by the HIV co-pandemic (70). The classical presentation of disease often is masked by the untreated HIV coinfection (70), but in principle the majority of humans have a well-developed capacity to contain the infection, so that the majority of the world's population infected with the tubercle bacillus is asymptomatic, and only ∼10% of individuals develop active disease. This tip of the iceberg nevertheless is key to continuing the tuberculosis contagion in human populations, because active disease is necessary for the transmission of tuberculosis. We propose that autophagy plays a dual role: It both protects against the microbe and guards against host-inflicted tissue destruction and active disease. In this model autophagy curbs tuberculosis transmission by helping maintain the majority of the infected population asymptomatic. Strategies aimed at pharmacological manipulation of autophagy may diminish tuberculosis spread and may prove vital in containing the emergence of the increasingly drug-resistant tuberculosis strains.

Materials and Methods

Mice and Infection. The transgenic Atg5$^{fl/fl}$ LysM-Cre^{+} (myeloid-specific Atg5 deletion) and Atg5$^{fl/fl}$ LysM-Cre^{-} mice have been characterized previously (34), and the autophagy defect in BMM has been documented extensively (6). LC3-GFP knockin transgenic mice (71) and p62$^{-/-}$ knockout mice (72) have been described previously. Mice were maintained under specific pathogen-free conditions. F1 progeny from Atg5$^{fl/fl}$ LysM-Cre × Atg5$^{fl/fl}$ crosses were genotyped for the presence (LysM-Cre^{+}) or absence (LysM-Cre) of the LysM-Cre allele by Transnetyx Inc. Infection studies were carried out using a murine respiratory infection model (73) and virulent *M. tuberculosis* H37Rv with modifications (74, 75) described in *SI Appendix*. The standard low dose resulted in the initial bacterial deposition ranging in independent experiments from 10e^{2}–10e^{3} cfu of *M. tuberculosis* per lung. The high dose had the deposition range of 10e^{4} cfu per lung. All experiments were approved by the Institutional Animal Care and Use Committee of the University of New Mexico Health Sciences Center, in accordance with the National Institutes of Health guidelines for use of live animals. The University of New Mexico Health Sciences Center is accredited by the American Association for Accreditation of Laboratory Animal Care.

Cells, Flow Cytometry, and Immunodetection. All cells were pretreated with Stain FcX (anti-CD16/32) (Biolegend) before being stained for CD14 (Sa14-2), F4/80 (BM8), IFN-γ (XMG1.2), IL-17A (TC11-18H10.1), CD11b (M1/70), DEC205

(NLDL-145), CD8 (53-6.7), CD86 (GL-1), Ly6G (1A8), CD25 (PC61), MHC II (M5/114.15.2) (Biolegend), CD19 (eBio1D3), TCRβ (H57-597), CD3e (145-2C11), CD44 (IM7), CD4 (GK1.5), CD1d (1B1), DEC205 (205yekta), CD4 (RM4-5), CD45 (30-F11), CD3 (17A2), F4/80 (BM8), CD11b (M1/70), B220 (RA3-6B2), CD8α (53-6.7), IL-12p35 (4D10p35), IL-1α (ALF-161), MCH II (M5/114.15.2), CD25 (PC61.5) (eBioscience), and Ly6G (1a8) (BD Biosciences). Caspase 1 activity was measured by flow cytometry using the FLICA caspase 1 reagent (FAM-YVAD-FMK) (Immunochemistry Technologies). Cells were incubated with 7-AAD for viability assessment. Secreted cytokines (IL-1α, IL-1β, CXCL1, CXCL2, and IL-12p70) were measured by ELISA (R&D Systems). For cytokine secretion, murine BMM, prepared as described (32), were stimulated with 5 ng/mL mouse IFN-γ and 1 μg/mL LPS, with autophagy agonist and antagonists rapamycin (Invivogen), 3-MA, and bafilomycin A1; chemical inhibitors brefeldin A (Biolegend), YVAD, and ALLN (Sigma); or IL-1RA (R&D Systems), all added 30 min before LPS and IFN-γ stimulation. For autophagy-dependent unconventional secretion of cytosolic cytokines as described (6), BMM were stimulated for 1 h with 250 μg/mL silica (MIN-U-SIL-15; US Silica) with starvation (Earle's balanced salt solution; EBSS, Atlanta Biologicals) to induce autophagy.

DTH and Cell-Mediated Immunity. Mice were infected i.p. with 5×10^6 bacillus Calmette–Guérin for 21 d and then were injected in separate footpads with 50 μL of the synthetic PPD (a mixture of five antigens: Dnak, GroEL, Rv009, Rv0569, and Rv0685) at 1.0 μg/mL in PBS or with PBS (control). DTH was assessed as described (38) by comparing swelling to a baseline value immediately after injection. Splenocytes (5.0×10^5 cells per well) were restimulated with the synthetic PPD adjusted for 2.0 μg/mL (Dnak and GroEL) or 4.0 μg/mL (Rv009, Rv0569, and Rv0685), and culture supernatants were assayed for IFN-γ, TNF-α, IL-4, and IL-17 secretion by ELISA (R&D Systems).

T-Cell Assays. Single-cell suspensions from whole lungs isolated from naive $Atg5^{fl/fl}$ LysM-Cre^+ and -Cre^- mice were cultured in RPMI 10% FBS and Cell Stimulation Mixture (phorbol 12-myristate 13-acetate and ionomycin plus brefeldin A and monensin) (eBioscience) for 4 h and were analyzed by flow cytometry. For in vitro polarization, naive $CD4^+$ T cells from spleens were sorted as $CD44^{low}CD4^+TCR\beta^+$ cells in a MoFlo high-speed cell sorter (Beckman Coulter). Sorted cells (5×10^5 cells per well) were incubated with plate-bound anti-CD3 antibody (76) and were stimulated with 20 ng/mL IL-6, 5 ng/mL TGF-β, 20 ng/mL IL-1α, or 20 ng/mL IL-1β (R&D Systems) in the presence of anti-CD28 (37.51), anti–IFN-γ (R4.6A2), anti–IL-4 (11B11), and anti–IL-2 (JE56-1A12) (eBioscience). After 4 d, cells were stimulated with 1× Cell Stimulation Mixture in the presence of protein transport inhibitors for 5 h at 37 °C and were analyzed by flow cytometry.

Other Experimental Procedures. Additional methods are described in *SI Appendix*.

ACKNOWLEDGMENTS. We thank Michal Mudd, Joshua Nguyen, Monique Nysus, Dennis Cook, and Charlene Hensler for assistance and Herbert Virgin for providing $Atg5^{Fl/Fl}$ LysM-Cre mice, which were generated by support from AI057160 Project 5. This work was supported by National Institutes of Health (NIH) Grants R01 AI069345 and R01 AI042999 and in part by National Center for Research Resources and National Center for Advancing Translational Sciences NIH Grant UL1 TR000041. E.F.C. was supported by a Supplement 3R01AI042999-13S1 from NIH. M.A.M. was supported by Training Grant T32AI007638 from NIH.

1. Mizushima N, Yoshimori T, Ohsumi Y (2011) The role of Atg proteins in autophagosome formation. *Annu Rev Cell Dev Biol* 27:107–132.
2. Mizushima N, Levine B, Cuervo AM, Klionsky DJ (2008) Autophagy fights disease through cellular self-digestion. *Nature* 451(7182):1069–1075.
3. Levine B, Mizushima N, Virgin HW (2011) Autophagy in immunity and inflammation. *Nature* 469(7330):323–335.
4. Narita M, et al. (2011) Spatial coupling of mTOR and autophagy augments secretory phenotypes. *Science* 332(6032):966–970.
5. Manjithaya R, Anjard C, Loomis WF, Subramani S (2010) Unconventional secretion of Pichia pastoris Acb1 is dependent on GRASP protein, peroxisomal functions, and autophagosome formation. *J Cell Biol* 188(4):537–546.
6. Dupont N, et al. (2011) Autophagy-based unconventional secretory pathway for extracellular delivery of IL-1β. *EMBO J* 30(23):4701–4711.
7. Deretic V, Jiang S, Dupont N (2012) Autophagy intersections with conventional and unconventional secretion in tissue development, remodeling and inflammation. *Trends in Cell Biology* 22(8):397–406.
8. He C, Levine B (2010) The Beclin 1 interactome. *Curr Opin Cell Biol* 22(2):140–149.
9. Tattoli I, et al. (2012) Amino acid starvation induced by invasive bacterial pathogens triggers an innate host defense program. *Cell Host Microbe* 11(6):563–575.
10. Criollo A, et al. (2011) Inhibition of autophagy by TAB2 and TAB3. *EMBO J* (vol/vol) 30 (24):4908–4920.
11. Lee HK, Lund JM, Ramanathan B, Mizushima N, Iwasaki A (2007) Autophagy-dependent viral recognition by plasmacytoid dendritic cells. *Science* 315(5817): 1398–1401.
12. Saitoh T, Akira S (2010) Regulation of innate immune responses by autophagy-related proteins. *J Cell Biol* 189(6):925–935.
13. Thurston TL, Wandel MP, von Muhlinen N, Foeglein A, Randow F (2012) Galectin 8 targets damaged vesicles for autophagy to defend cells against bacterial invasion. *Nature* 482(7385):414–418.
14. Deretic V (2012) Autophagy: An emerging immunological paradigm. *J Immunol* 189 (1):15–20.
15. Jounai N, et al. (2011) NLRP4 negatively regulates autophagic processes through an association with beclin1. *J Immunol* 186(3):1646–1655.
16. Tal MC, et al. (2009) Absence of autophagy results in reactive oxygen species-dependent amplification of RLR signaling. *Proc Natl Acad Sci USA* 106(8):2770–2775.
17. Xu Y, et al. (2007) Toll-like receptor 4 is a sensor for autophagy associated with innate immunity. *Immunity* 27(1):135–144.
18. Delgado MA, Elmaoued RA, Davis AS, Kyei G, Deretic V (2008) Toll-like receptors control autophagy. *EMBO J* 27(7):1110–1121.
19. Travassos LH, et al. (2010) Nod1 and Nod2 direct autophagy by recruiting ATG16L1 to the plasma membrane at the site of bacterial entry. *Nat Immunol* 11(1):55–62.
20. Lee HK, et al. (2010) In vivo requirement for Atg5 in antigen presentation by dendritic cells. *Immunity* 32(2):227–239.
21. Jia W, Pua HH, Li QJ, He YW (2011) Autophagy regulates endoplasmic reticulum homeostasis and calcium mobilization in T lymphocytes. *J Immunol* 186(3):1564–1574.
22. Harris J, et al. (2007) T helper 2 cytokines inhibit autophagic control of intracellular Mycobacterium tuberculosis. *Immunity* 27(3):505–517.
23. Zhou R, Yazdi AS, Menu P, Tschopp J (2011) A role for mitochondria in NLRP3 inflammasome activation. *Nature* 469(7329):221–225.
24. Nakahira K, et al. (2011) Autophagy proteins regulate innate immune responses by inhibiting the release of mitochondrial DNA mediated by the NALP3 inflammasome. *Nat Immunol* 12(3):222–230.
25. Shi CS, et al. (2012) Activation of autophagy by inflammatory signals limits IL-1β production by targeting ubiquitinated inflammasomes for destruction. *Nat Immunol* 13(3):255–263.
26. Gutierrez MG, et al. (2004) Autophagy is a defense mechanism inhibiting BCG and Mycobacterium tuberculosis survival in infected macrophages. *Cell* 119(6):753–766.
27. Alonso S, Pethe K, Russell DG, Purdy GE (2007) Lysosomal killing of Mycobacterium mediated by ubiquitin-derived peptides is enhanced by autophagy. *Proc Natl Acad Sci USA* 104(14):6031–6036.
28. Yuk JM, et al. (2009) Vitamin D3 induces autophagy in human monocytes/macrophages via cathelicidin. *Cell Host Microbe* 6(3):231–243.
29. Kim JJ, et al. (2012) Host cell autophagy activated by antibiotics is required for their effective antimycobacterial drug action. *Cell Host Microbe* 11(5):457–468.
30. Nakagawa I, et al. (2004) Autophagy defends cells against invading group A Streptococcus. *Science* 306(5698):1037–1040.
31. Deretic V (2012) Autophagy as an innate immunity paradigm: Expanding the scope and repertoire of pattern recognition receptors. *Curr Opin Immunol* 24(1):21–31.
32. Ponpuak M, et al. (2010) Delivery of cytosolic components by autophagic adaptor protein p62 endows autophagosomes with unique antimicrobial properties. *Immunity* 32(3):329–341.
33. Vergne I, Chua J, Singh SB, Deretic V (2004) Cell biology of mycobacterium tuberculosis phagosome. *Annu Rev Cell Dev Biol* 20:367–394.
34. Zhao Z, et al. (2008) Autophagosome-independent essential function for the autophagy protein Atg5 in cellular immunity to intracellular pathogens. *Cell Host Microbe* 4(5):458–469.
35. Flynn JL, Chan J (2001) Immunology of tuberculosis. *Annu Rev Immunol* 19:93–129.
36. Korn T, Bettelli E, Oukka M, Kuchroo VK (2009) IL-17 and Th17 Cells. *Annu Rev Immunol* 27:485–517.
37. Chung Y, et al. (2009) Critical regulation of early Th17 cell differentiation by interleukin-1 signaling. *Immunity* 30(4):576–587.
38. Yang H, et al. (2011) Three protein cocktails mediate delayed-type hypersensitivity responses indistinguishable from that elicited by purified protein derivative in the guinea pig model of Mycobacterium tuberculosis infection. *Infect Immun* 79(2): 716–723.
39. Mayer-Barber KD, et al. (2011) Innate and adaptive interferons suppress IL-1α and IL-1β production by distinct pulmonary myeloid subsets during Mycobacterium tuberculosis infection. *Immunity* 35(6):1023–1034.
40. Jain A, et al. (2010) p62/SQSTM1 is a target gene for transcription factor NRF2 and creates a positive feedback loop by inducing antioxidant response element-driven gene transcription. *J Biol Chem* 285(29):22576–22591.
41. Moscat J, Diaz-Meco MT (2009) p62 at the crossroads of autophagy, apoptosis, and cancer. *Cell* 137(6):1001–1004.
42. Mathew R, et al. (2009) Autophagy suppresses tumorigenesis through elimination of p62. *Cell* 137(6):1062–1075.
43. Xia Y, et al. (1999) RelB modulation of IkappaBalpha stability as a mechanism of transcription suppression of interleukin-1alpha (IL-1alpha), IL-1beta, and tumor necrosis factor alpha in fibroblasts. *Mol Cell Biol* 19(11):7688–7696.
44. Fettelschoss A, et al. (2011) Inflammasome activation and IL-1β target IL-1α for secretion as opposed to surface expression. *Proc Natl Acad Sci USA* 108(44): 18055–18060.
45. Keller M, Rüegg A, Werner S, Beer HD (2008) Active caspase-1 is a regulator of unconventional protein secretion. *Cell* 132(5):818–831.

46. Gross O, et al. (2012) Inflammasome activators induce interleukin-1α secretion via distinct pathways with differential requirement for the protease function of caspase-1. *Immunity* 36(3):388–400.
47. Li Y, Arnold JM, Pampillo M, Babwah AV, Peng T (2009) Taurine prevents cardiomyocyte death by inhibiting NADPH oxidase-mediated calpain activation. *Free Radic Biol Med* 46(1):51–61.
48. Sharma AK, Rohrer B (2007) Sustained elevation of intracellular cGMP causes oxidative stress triggering calpain-mediated apoptosis in photoreceptor degeneration. *Curr Eye Res* 32(3):259–269.
49. Sorimachi H, Hata S, Ono Y (2011) Impact of genetic insights into calpain biology. *J Biochem* 150(1):23–37.
50. Kim BH, et al. (2011) A family of IFN-γ-inducible 65-kD GTPases protects against bacterial infection. *Science* 332(6030):717–721.
51. Hartman ML, Kornfeld H (2011) Interactions between naïve and infected macrophages reduce Mycobacterium tuberculosis viability. *PLoS ONE* 6(11):e27972.
52. Thurston TL, Ryzhakov G, Bloor S, von Muhlinen N, Randow F (2009) The TBK1 adaptor and autophagy receptor NDP52 restricts the proliferation of ubiquitin-coated bacteria. *Nat Immunol* 10(11):1215–1221.
53. Dupont N, et al. (2009) Shigella phagocytic vacuolar membrane remnants participate in the cellular response to pathogen invasion and are regulated by autophagy. *Cell Host Microbe* 6(2):137–149.
54. Yoshikawa Y, et al. (2009) Listeria monocytogenes ActA-mediated escape from autophagic recognition. *Nat Cell Biol* 11(10):1233–1240.
55. Wild P, et al. (2011) Phosphorylation of the autophagy receptor optineurin restricts Salmonella growth. *Science* 333(6039):228–233.
56. Orvedahl A, et al. (2010) Autophagy protects against Sindbis virus infection of the central nervous system. *Cell Host Microbe* 7(2):115–127.
57. Cadwell K, et al. (2010) Virus-plus-susceptibility gene interaction determines Crohn's disease gene Atg16L1 phenotypes in intestine. *Cell* 141(7):1135–1145.
58. Saitoh T, et al. (2008) Loss of the autophagy protein Atg16L1 enhances endotoxin-induced IL-1beta production. *Nature* 456(7219):264–268.
59. Torrado E, Cooper AM (2010) IL-17 and Th17 cells in tuberculosis. *Cytokine Growth Factor Rev* 21(6):455–462.
60. Pedrosa J, et al. (2000) Neutrophils play a protective nonphagocytic role in systemic Mycobacterium tuberculosis infection of mice. *Infect Immun* 68(2):577–583.
61. Seiler P, et al. (2003) Early granuloma formation after aerosol Mycobacterium tuberculosis infection is regulated by neutrophils via CXCR3-signaling chemokines. *Eur J Immunol* 33(10):2676–2686.
62. Khader SA, et al. (2007) IL-23 and IL-17 in the establishment of protective pulmonary CD4+ T cell responses after vaccination and during Mycobacterium tuberculosis challenge. *Nat Immunol* 8(4):369–377.
63. Desvignes L, Ernst JD (2009) Interferon-gamma-responsive nonhematopoietic cells regulate the immune response to Mycobacterium tuberculosis. *Immunity* 31(6): 974–985.
64. Nandi B, Behar SM (2011) Regulation of neutrophils by interferon-γ limits lung inflammation during tuberculosis infection. *J Exp Med* 208(11):2251–2262.
65. Cruz A, et al. (2010) Pathological role of interleukin 17 in mice subjected to repeated BCG vaccination after infection with Mycobacterium tuberculosis. *J Exp Med* 207(8): 1609–1616.
66. Berry MP, et al. (2010) An interferon-inducible neutrophil-driven blood transcriptional signature in human tuberculosis. *Nature* 466(7309):973–977.
67. Desvignes L, Wolf AJ, Ernst JD (2012) Dynamic roles of type I and type II IFNs in early infection with Mycobacterium tuberculosis. *J Immunol* 188(12):6205–6215.
68. Harris J, et al. (2011) Autophagy controls IL-1{beta} secretion by targeting pro-IL-1 {beta} for degradation. *J Biol Chem* 286(11):9587–9597.
69. Cadwell K, et al. (2008) A key role for autophagy and the autophagy gene Atg16l1 in mouse and human intestinal Paneth cells. *Nature* 456(7219):259–263.
70. Nunn P, et al. (2005) Tuberculosis control in the era of HIV. *Nat Rev Immunol* 5(10): 819–826.
71. Mizushima N, Yamamoto A, Matsui M, Yoshimori T, Ohsumi Y (2004) In vivo analysis of autophagy in response to nutrient starvation using transgenic mice expressing a fluorescent autophagosome marker. *Mol Biol Cell* 15(3):1101–1111.
72. Komatsu M, et al. (2007) Homeostatic levels of p62 control cytoplasmic inclusion body formation in autophagy-deficient mice. *Cell* 131(6):1149–1163.
73. Flynn J, Tsenova L, Izzo A, Kaplan G (2008) Experimental animal models of tuberculosis. *Handbook of Tuberculosis: Immunology and Cell Biology*, eds Kaufmann S, Britton W (Wiley-VCH, Weinheim, Germany), pp 389–4226.
74. Talaat AM, Lyons R, Howard ST, Johnston SA (2004) The temporal expression profile of Mycobacterium tuberculosis infection in mice. *Proc Natl Acad Sci USA* 101(13): 4602–4607.
75. Zahrt TC, Deretic V (2001) Mycobacterium tuberculosis signal transduction system required for persistent infections. *Proc Natl Acad Sci USA* 98(22):12706–12711.
76. Hu W, Troutman TD, Edukulla R, Pasare C (2011) Priming microenvironments dictate cytokine requirements for T helper 17 cell lineage commitment. *Immunity* 35(6): 1010–1022.